

ELECTROMAGNETIC SCATTERING FROM CONDUCTING CIRCULAR CYLINDER COATED BY METAMATERIALS AND LOADED WITH HELICAL STRIPS UNDER OBLIQUE INCIDENCE

L. K. Hady and A. A. Kishk

Department of Electrical Engineering
Center for Applied Electromagnetic System Research
University of Mississippi
University, MS 38677, USA

Abstract—The asymptotic strip boundary condition (ASBC) is applied to analyze the solution of the electromagnetic scattering from a conducting cylinder coated with a homogeneous linear material layer and loaded with conducting helical strips. Such homogeneous material layer can be implemented by a conventional dielectric material, a single negative (SNG) or double negative (DNG) meta-material layer. A study of different materials' constitutive parameters is presented with accordance to Drude and Lorentz material modeling. The boundary condition assumes that the strips are rounded around the coated cylinder in a helical form and both the strip's period and the spacing between the helix turns are very small and mathematically approaching the zero. Scattering due to normal and oblique incident plane waves (θ_i , ϕ_i) of arbitrary polarization using the series solution is also computed. A number of parametric studies were investigated to illustrate the advantages of using metamaterials compared with conventional coating materials in terms of strip's rounding pitch angle and coating layer electrical thickness variations. It is also shown that for SNG materials, modified Bessel functions are used to accept negative arguments. Coating with metamaterials proves to achieve higher forward scattering compared with conventional materials for the same electrical coating thickness.

1. INTRODUCTION

Strip periodic surfaces, polarization selective reflecting or transmitting surfaces [1, 2], exhibit superior and attractive properties to be used in

antenna applications such as in circular waveguide and horn antenna designs to improve their radiation characteristics [3, 4]. It has been reported in the literature that metal-conducting strips can replace the corrugations on the waveguide walls to realize both hard and soft surfaces [5, 6]. Such advantage helps in having an alternative inexpensive process and in reducing the forward scattering from the struts in the design of the reflector antenna struts [7, 8].

The asymptotic strip boundary condition (ASBC) was applied to analyze scattering from planar [6], arbitrarily shaped cylindrical structures loaded with conducting strips [9–11] based on expanding the scattered field on both sides of the grating in the Floquet modes then applying an approximation directly to the boundary conditions such that the tangential E-field is zero at the surface of each strip and continuous between the strips. As an alternative solution, the ASBC does not suffer from any geometrical limitations compared with the Floquet mode solution. It is applicable and easier to be implemented in computer programs for scattering or radiation calculations based on any numerical technique. This boundary condition becomes more accurate the smaller the period between the strips is in terms of the wavelength and is expected to be asymptotically exact when the strip period approaches to zero.

The concept of double negative (DNG) metamaterials [12–17], artificial materials, has increasingly received considerable attention and intensive interest due to the attractive theoretical predicted properties of these materials such as the reversal of the Snell's law, Doppler Effect and the backward Cherenkov radiation [18–22]. It was first postulated by Veslago in the 1967 [23] when he theoretically examined the propagation of plane waves in hypothetical medium with simultaneously negative real permittivity and real permeability and remarkably demonstrated that having media with both constitutive parameters are negative would lead to opposite directions of the Poynting vector; at the direction of energy propagation and group velocity; and phase velocity due to the existence of backward waves propagating. They are also known as left-handed (LH) materials due to the left-handed dyad formed by the electric, magnetic and wave vector components. Theoretical studies and experimental demonstrations have been successfully developed by research groups worldwide for the use of metamaterials in RF circuit design and antenna size reduction [23–27]. Special attention has been paid to metamaterials with single negative (SNG) material parameter such as the epsilon-negative (ENG) and mu-negative (MNG) materials to overcome microwave and optical applications' physical limitations. It was found that SNG media support evanescent waves within certain

frequency range and possess advantageous characteristics than the DNG materials in scattering and guiding when they are paired in suitable conjugate manner for future applications [12, 28–29].

Significant theoretical and experimental efforts have focused on studying the dispersive nature of metamaterials after Veslago. It was found that both Drude and Lorentz models could reasonably describe the dispersive behavior of both permeability and permittivity of DNG materials in a narrow frequency band where metamaterials' constitutive parameters are inherently frequency dependent [28–30]. For this reason, such behavior must be taken into consideration in choosing the suitable constitutive parameters for such materials at the designed frequency.

In this paper, we will present a simple concept to analyze strip periodic surfaces. The solution may be valid for low frequency applications or when the number of periods per wavelength is very large and on the limit of the periods approaching to zero. This concept can be applied in any coordinate system, i.e., it is not restricted to any geometry while it can also be mixed with other boundary conditions to analyze composite structures where periodic strips are parts of the object. Here we are applying this concept to circular structures in order to obtain analytic series solution, while in other cases it will not be possible to analyze without numerical solutions for surface integral equations. Tremendous work was done to study the electromagnetic scattering from conducting cylinders with coating materials and can be found in literature [31–40]. The objective of this paper is to study the scattering from a conducting cylinder coated with a metamaterials layer and loaded with conducting helical strips by using the ASBC. The constitutive parameters of such SNG or DNG material layer are chosen to satisfy the frequency dependence equations stated in both Drude and Lorentz models at the given frequency. The present work is proved to be valid implementation of the ASBC with other numerical techniques. The boundary condition is expected to be asymptotically correct when we have zero spacing between the helix turns while the strips are rounded around the coated cylinder in a helical form with very small strip's period. Excellent agreement and further validation are done when both longitudinal (z -directed) and circumferential (ϕ -directed) strip loading are used as special cases. These results are removed for brevity.

2. FORMULATION

Consider a perfectly conducting circular cylinder of a radius b coated with a uniform homogenous isotropic material layer of radius a as

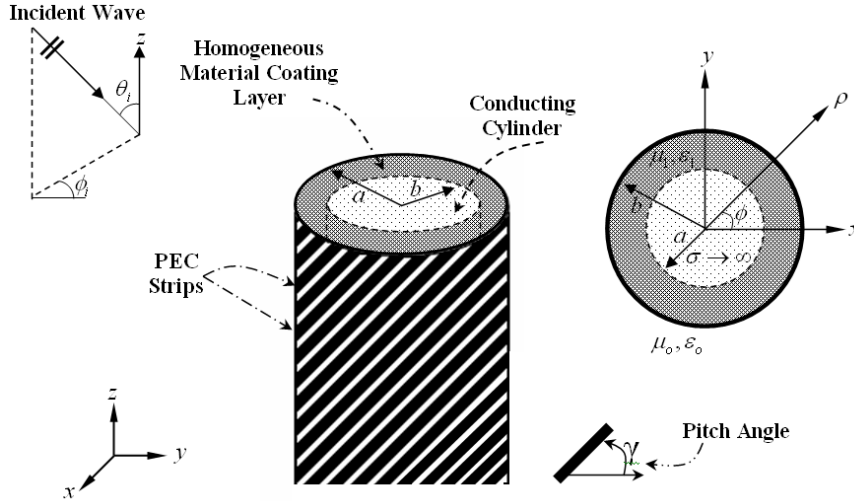


Figure 1. Geometry of Conducting Cylinder coated with a homogenous linear material and loaded with conducting helical strips.

shown in Fig. 1. The material coating can be implemented as a conventional dielectric material, a single negative (SNG) or double negative (DNG) metamaterials layer with a general permittivity ϵ_1 and permeability μ_1 . A helical periodic conducting strip of a very small spacing between the turns compared with the wavelength loads the surface of the coated layer at a pitch angle γ with the xy plane. Variations between $\gamma = 0^\circ$ and $\gamma = 90^\circ$ will be included in the forthcoming analysis as special cases for further verifications as when $\gamma = 0^\circ$, the strips will be ϕ -directed and when $\gamma = 90^\circ$, the strips will be z -directed. The excitation is assumed to be a plane wave obliquely incident on the object with an angle of incidence θ_i measured from the z -axis and ϕ_i measured from the x -axis in the xy plane. The incident fields can be expressed as:

$$E^{inc} = -E_o \left(\cos \alpha \hat{\theta} + \sin \alpha \hat{\phi} \right) e^{-jk_e \hat{k} \cdot r} \quad (1)$$

$$H^{inc} = \left(\hat{k} \times E^{inc} \right) / \eta_o \quad (2)$$

with

$$\hat{\theta}(\theta_i, \phi_i) = \hat{x} \cos \theta_i \cos \phi_i + \hat{y} \cos \theta_i \sin \phi_i - \hat{z} \sin \theta_i \quad (3)$$

$$\hat{\phi}(\phi_i) = -\hat{x} \sin \phi_i + \hat{y} \cos \phi_i \quad (4)$$

where the polarization angle α is the angle the incident electric field makes with the plane of incidence. If $\alpha = 0$, the plane is TM_z polarized

and if $\alpha = \pi/2$, the plane wave is TE_z polarized. The quantity E_o is the amplitude of the incident electric field, $\hat{k} = \hat{r}(\theta_i, \phi_i)$ is a unit vector pointing in the direction of propagation, k_e is the wave number in free space and \hat{x} , \hat{y} and \hat{z} are the unit vectors in the directions of x , y and z , respectively and $\hat{r}(\theta_i, \phi_i)$, $\hat{\theta}(\theta_i, \phi_i)$ and $\hat{\phi}(\phi_i)$ are the unit vectors in the directions of r , θ_i and ϕ_i in the spherical coordinate system. The z -component of the incident field can be expanded in the cylindrical coordinate system (ρ, ϕ, z) according to [9]:

$$\begin{Bmatrix} E_z^i \\ H_z^i \end{Bmatrix} = \frac{\kappa E_o}{k_e} e^{j\tau z} \begin{Bmatrix} \cos \alpha \\ \sin \alpha / \eta_o \end{Bmatrix} \sum_{n=-\infty}^{\infty} j^{-n} J_n(\kappa \rho) e^{jn(\phi-\phi_i)} \quad (5)$$

where $\kappa = k_e \sin \theta_i$, $\tau = k_e \cos \theta_i$ and $J_n(x)$ is the Bessel function of order n . From Maxwell's equations, the other incident field components can be expressed as:

$$\begin{Bmatrix} E_\phi^i \\ H_\phi^i \end{Bmatrix} = j \frac{k_e}{\kappa} E_o e^{j\tau z} \times \sum_{n=-\infty}^{\infty} j^{-n} \left[j \frac{n\tau}{k_e^2 \rho} \begin{Bmatrix} \cos \alpha \\ \sin \alpha / \eta \end{Bmatrix} J_n(\kappa \rho) \right. \\ \left. + \frac{1}{k_e} \begin{Bmatrix} \sin \alpha \\ -\cos \alpha / \eta \end{Bmatrix} J'_n(\kappa \rho) \right] e^{jn(\phi-\phi_i)} \quad (6)$$

where $J'_n(x)$ is the derivative of the Bessel function $J_n(x)$ with respect to the whole argument. All the field components can be obtained from the z -components of the electric and magnetic fields and expressed in terms of unknown coefficients. The z -component of the scattered fields can be expressed as:

$$\begin{Bmatrix} E_z^s \\ H_z^s \end{Bmatrix} = E_o e^{j\tau z} \sum_{n=-\infty}^{\infty} \begin{Bmatrix} a_n \\ b_n \end{Bmatrix} j^{-n} H_n^{(2)}(\kappa \rho) e^{jn(\phi-\phi_i)} \quad \rho \geq a \quad (7)$$

where $H_n^{(2)}(x)$ is the Hankel function of the second kind and of order n . Again from Maxwell's equations the rest of the scattered field components can be obtained as:

$$\begin{Bmatrix} E_\phi^s \\ H_\phi^s \end{Bmatrix} = j \frac{k_e}{\kappa^2} E_o e^{j\tau z} \times \sum_{n=-\infty}^{\infty} j^{-n} \left[j \frac{n\tau}{k_e \rho} \begin{Bmatrix} a_n \\ b_n \end{Bmatrix} H_n^{(2)}(\kappa \rho) \right. \\ \left. + \begin{Bmatrix} \eta b_n \\ -a_n / \eta \end{Bmatrix} H_n'^{(2)}(\kappa \rho) \right] e^{jn(\phi-\phi_i)}$$

Similarly we can get the components of the diffracted fields inside the coated layer as follows:

$$\begin{Bmatrix} E_\phi^d \\ H_\phi^d \end{Bmatrix} = j \frac{k_d}{\kappa_d^2} E_o e^{j\tau z} \times \sum_{n=-\infty}^{\infty} j^{-n} \left[j \frac{n\tau}{k_d \rho} \left[\begin{Bmatrix} c_n \\ d_n \end{Bmatrix} J_n(\kappa_d \rho) + \begin{Bmatrix} e_n \\ f_n \end{Bmatrix} H_n^{(2)}(\kappa_d \rho) \right] \right]$$

$$+ \left[\left\{ \frac{\eta_d d_n}{c_n / \eta_d} \right\} J'_n(\kappa_d \rho) + \left\{ \frac{\eta_d f_n}{e_n / \eta_d} \right\} H_n^{(2)}(\kappa_d \rho) \right] e^{jn(\phi - \phi_i)} \quad (8)$$

Again the prime denotes the derivative with respect to the whole argument. For the ϕ -variation, the exponential function is used because of the helix disturbs the periodic behavior of ϕ while a sine/cosine form of variations is used when $\gamma = 0^\circ$ and $\gamma = 90^\circ$ to describe special strip loadings. It is important to mention that a modified Bessel function and its derivative for complex argument are programmed to take care of the negative sign that show up for the SNG material analysis. In other words, for both DNG and DPS materials, the usual Bessel function with its derivative can be used for the complex argument. The boundary conditions will be assumed that the tangential electric field along the conducting strips vanishes on the surface from inside and outside the coated material layer surface. Therefore,

$$\cos \gamma (E_\phi^i + E_\phi^s) + \sin \gamma (E_z^i + E_z^s) = 0 \quad \text{at } \rho = a \quad (9)$$

$$\cos \gamma E_\phi^d + \sin \gamma E_z^d = 0 \quad \text{at } \rho = a \quad (10)$$

On the other hand the electric field components normal to the strips and the magnetic field along the strips are continuous across the surface. Therefore,

$$\cos \gamma (E_z^i + E_z^s) - \sin \gamma (E_\phi^i + E_\phi^s) = \cos \gamma E_z^d - \sin \gamma E_\phi^d \quad (11)$$

$$\cos \gamma (H_\phi^i + H_\phi^s) + \sin \gamma (H_z^i + H_z^s) = \cos \gamma H_\phi^d + \sin \gamma H_z^d \quad (12)$$

On the conducting core the tangential field components will vanish as:

$$E_z^d = 0 \quad \text{at } \rho = b \quad (13)$$

$$E_\phi^d = 0 \quad \text{at } \rho = b \quad (14)$$

From the previous boundary conditions, the unknown field expansion coefficients can be obtained as follows:

$$a_n = \frac{1}{ak_{d\rho}^2 k_o H_n^{(2)}(k_o \rho a)} \left\{ k_o \cos \gamma (nk_z \sin \gamma + k_{d\rho}^2 a \cos \gamma) [J_n(k_{d\rho} a) c_n + H_n^{(2)}(k_{d\rho} a) e_n] \right. \\ \left. - j k_o k_{d\rho} \mu_d \omega a \cos \gamma \sin \gamma [J'_n(k_{d\rho} a) d_n + H_n^{(2)'}(k_{d\rho} a) f_n] \right. \\ \left. - ak_{d\rho}^3 \cos \alpha J_n(k_o \rho a) \right\}$$

$$\begin{aligned}
b_n &= \frac{j}{\omega a^2 \mu_o k_{d\rho}^2 k_{o\rho} H_n^{(2)}(k_{o\rho} a)} \left\{ \left(\sin \gamma \cos \gamma \left(k_{d\rho}^2 k_{o\rho}^2 a^2 - n k_z^2 \right) \right. \right. \\
&\quad \left. \left. - n a k_z \left(k_{d\rho}^2 \cos^2 \gamma - k_{o\rho}^2 \sin^2 \gamma \right) \right) \left[J_n(k_{d\rho} a) c_n + H_n^{(2)}(k_{d\rho} a) e_n \right] \right. \\
&\quad \left. + j a \omega \mu_d k_{d\rho} \sin \gamma \left(n k_z \cos \gamma - k_{o\rho}^2 a \sin \gamma \right) \right. \\
&\quad \left. \left[J_n'(k_{d\rho} a) d_n + H_n^{(2)}(k_{d\rho} a) f_n \right] + j k_{d\rho}^2 k_{o\rho}^2 a^2 \sin \alpha J_n'(k_{o\rho} a) \right\} \\
c_n &= \frac{-H_n^{(2)}(k_{d\rho} b)}{J_n(k_{d\rho} b)} e_n \\
d_n &= -\frac{H_n^{(2)}(k_{d\rho} b)}{J_n'(k_{d\rho} b)} f_n \\
e_n &= \frac{2\omega \mu_d k_{o\rho} k_{d\rho}^3 \cos \gamma}{\pi D} J_n(k_{d\rho} b) \chi_1 \left\{ \left(n k_z \cos \gamma - a k_{o\rho}^2 \sin \gamma \right) \right. \\
&\quad \left. \sin \alpha H_n^{(2)}(k_{o\rho} a) - j a k_o k_{o\rho} \cos \alpha \cos \gamma H_n^{(2)}(k_{o\rho} a) \right\} \\
f_n &= \frac{-2j k_{o\rho} k_{d\rho}^2 \left(n k_z \cos \gamma - a k_{d\rho}^2 \sin \gamma \right)}{\pi a D} J_n'(k_{d\rho} b) \chi_2 \\
&\quad \left\{ \sin \alpha \left(n k_z \cos \gamma - a k_{o\rho}^2 \sin \gamma \right) H_n^{(2)}(k_{o\rho} a) \right. \\
&\quad \left. - j a k_o k_{o\rho} \cos \alpha \cos \gamma H_n^{(2)}(k_{o\rho} a) \right\}
\end{aligned}$$

where:

$$\begin{aligned}
D &= \omega \chi_2 H_n^{(2)}(k_{o\rho} a) \left[\mu_o k_{o\rho}^3 \chi_3 \psi_d^2 H_n^{(2)}(k_{o\rho} a) + \mu_d k_{d\rho}^3 \chi_1 \psi_o^2 H_n^{(2)}(k_{o\rho} a) \right] \\
&\quad + a^2 k_{d\rho}^2 k_{o\rho}^2 k_d k_o \chi_1 \cos^2 \gamma H_n^{(2)}(k_{o\rho} a) \\
&\quad \left[\eta_o k_d k_{o\rho} \chi_4 H_n^{(2)}(k_{o\rho} a) - \eta_d k_o k_{d\rho} \chi_2 H_n^{(2)}(k_{o\rho} a) \right] \\
\chi_1 &= J_n'(k_{d\rho} a) H_n^{(2)}(k_{d\rho} b) - J_n'(k_{d\rho} b) H_n^{(2)}(k_{d\rho} a) \\
\chi_2 &= J_n(k_{d\rho} a) H_n^{(2)}(k_{d\rho} b) - J_n(k_{d\rho} b) H_n^{(2)}(k_{d\rho} a) \\
\chi_3 &= J_n'(k_{d\rho} b) H_n^{(2)}(k_{d\rho} a) - J_n(k_{d\rho} a) H_n^{(2)}(k_{d\rho} b) \\
\chi_4 &= J_n'(k_{d\rho} a) H_n^{(2)}(k_{d\rho} b) - J_n(k_{d\rho} b) H_n^{(2)}(k_{d\rho} a) \\
\psi_d &= n k_z \cos \gamma - a k_{d\rho}^2 \sin \gamma \\
\psi_o &= n k_z \cos \gamma - a k_{o\rho}^2 \sin \gamma
\end{aligned}$$

Due to phase matching, the wave number components in both free space and the coating material can be defined as $k_z = k_{oz} = k_{dz} = k_o \cos \theta_{in}$, $k_{o\rho} = k_o \sin \theta_{in}$ and $k_{d\rho} = k_o \sqrt{\mu_d \varepsilon_d - \cos^2 \theta_{in}}$,

respectively. For SNG materials where either the material permittivity or permeability has a negative real part, the wave number $k_{d\rho}$ will be of negative value and that mainly leads to the use of modified special Bessel functions of first and second type to replace the $J_n(x)$, and $H_n(x)$, respectively for accurate analysis of large complex arguments.

3. EFFECTIVE MATERIAL PARAMETERS AND DISPERSION MODELS

Remarkable studies were done after Veslago in 1960s [23] concerning the behavior of the new artificial engineered materials. In general, DNG materials possess simultaneously negative effective permittivity and permeability which can be obtained from a periodic array of thin metallic wires; that creates negative permittivity medium, combined with an array of split ring resonators (SRR) to create the negative permeability medium [18, 28–30]. Several material models had been proposed to describe the dispersive nature of metamaterials and their frequency dependence [40–47]. Both Drude and Lorentz models were reasonably used to determine the effective constitutive parameters of SNG and DNG materials as a function of frequency [48, 49]. They are preferred than other models because their equations stems to replace the material's atoms and molecules by harmonic oscillators influenced by any frequency perturbation near the resonant frequency within a narrow range. It is remarkably noticed that passive metamaterials are inherently dispersive in a narrow frequency band where they have simultaneously negative permittivity and permeability. The standard Drude-Lorentz model equations can be stated as follows [42]:

$$\varepsilon_{eff}(\omega) = \varepsilon_{\infty} - \frac{\omega_p^2}{\omega(\omega - i\nu_c)} \quad \text{and} \quad \mu_{eff} = \mu_{\infty} + \frac{(\mu_s - \mu_{\infty})\omega_o^2}{\omega_o^2 + i\omega\delta - \omega^2} \quad (15)$$

The above parameters were chosen carefully to get different material behavior at different frequency ranges with distinct effective constitutive parameters as shown in Fig. 2 and stated in Table 1:

From the assumed material parameters, different media were obtained at different frequencies as stated in Table 2, which will be used later on to verify the behavior of the studied structure with different materials.

4. NUMERICAL RESULTS

The above equations have been implemented in a FORTRAN code. To verify the code, numerical solution using the method of moments

Table 1. Drude-Lorentz model parameters.

| Parameter | Definition | Value |
|-------------------|---|---------------------------|
| ϵ_∞ | electric permittivity at the high frequency limit | 2.2 |
| ω_p | radial plasma frequency | $2\pi(14.63 \times 10^9)$ |
| ν_c | the collision frequency | 30.69×10^6 |
| μ_s | magnetic permittivity at low frequency limit | 1.26 |
| ω_o | radial resonant frequency | $2\pi(9.5 \times 10^9)$ |
| μ_∞ | magnetic permittivity at high frequency limit | 1.05 |
| δ | Damping factor | 1.24×10^9 |

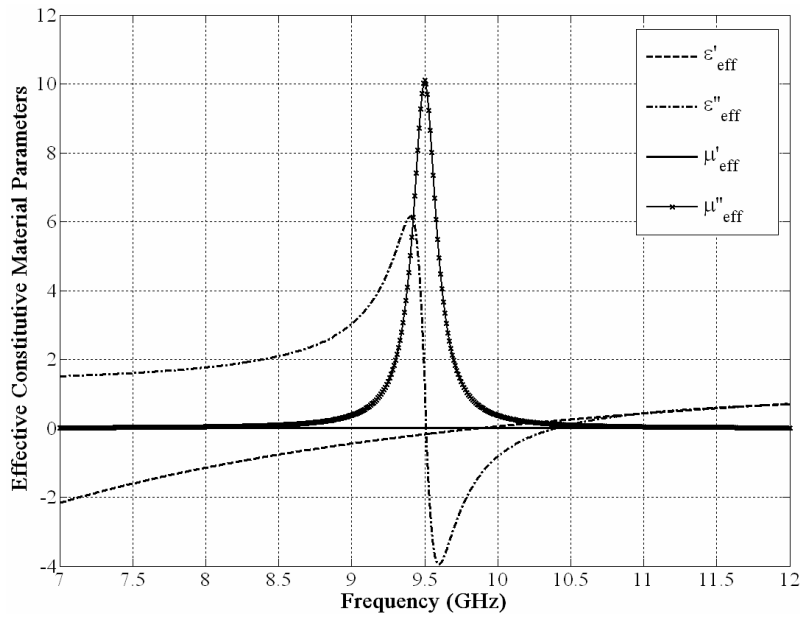


Figure 2. Effective electric permittivity $\epsilon_{eff} = \epsilon' - j\epsilon''$ and effective permeability $\mu_{eff} = \mu' - j\mu''$ for the proposed Drude and Lorentz material modeling parameters.

(MOM) code was used and both solutions proved to have excellent agreement. The scattering from the conducting circular cylinder coated with different material types and loaded with helical strips in the two main polarization were also obtained where the polarization angle α may have the value of 0° and 90° to achieve TM_z and TE_z polarizations respectively. Fig. 3 shows the scattering from the structure described

Table 2. Different material types with respect to frequency dependence.

| Frequency (GHz) | $\epsilon_{eff} = \epsilon' - j\epsilon''$ | $\mu_{eff} = \mu' - j\mu''$ | Material Type |
|-----------------|--|-----------------------------|---------------|
| 9 | $-0.4424 - j0.0014$ | $3.0261 - j0.3794$ | ENG |
| 9.6 | $-0.1224 - j0.0012$ | $-3.9516 - j4.9612$ | DNG |
| 10.2 | $0.1427 - j0.001$ | $-0.2957 - j0.1964$ | MNG |
| 11 | $0.4311 - j0.0008$ | $0.4367 - j0.0433$ | DPS |

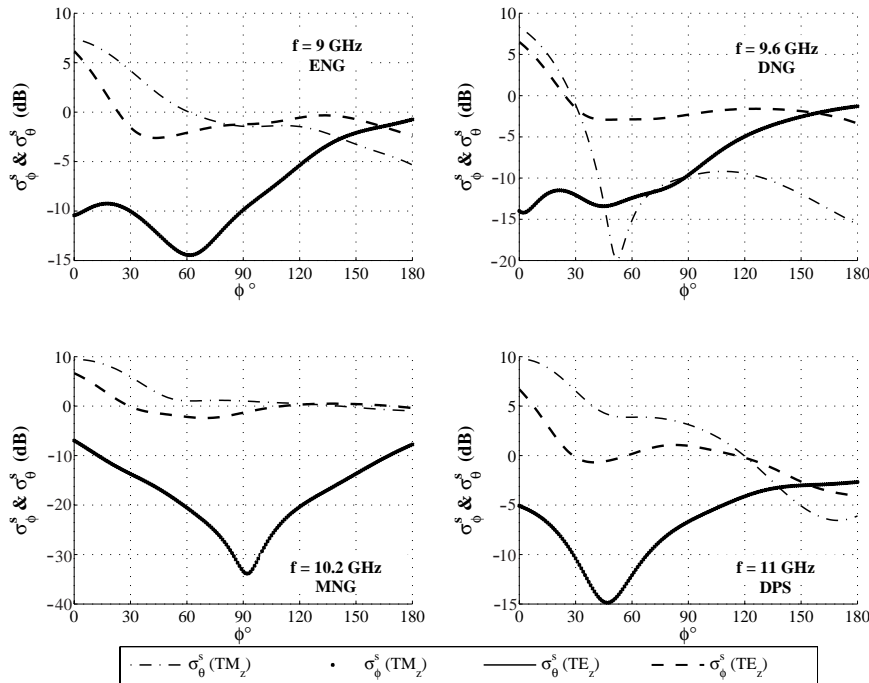


Figure 3. Scattering from a conducting cylinder coated with different materials of inner and outer radii $b = 1.2$ mm and $a = 1.5$ mm loaded with helical strips under oblique incidence ($\theta_i = 45^\circ$, $\phi_i = 0^\circ$).

previously in Fig. 1 with oblique incidence of $\theta_i = 45^\circ$ where the conducting cylinder radius and the coated layer's outer radius are $b = 1.2$ mm and $a = 1.5$ mm, respectively. The strips in this case are aligned with pitch angle $\gamma = 45^\circ$. The results in Fig. 3 were obtained in terms of the radar cross section (RCS) as well as all the following

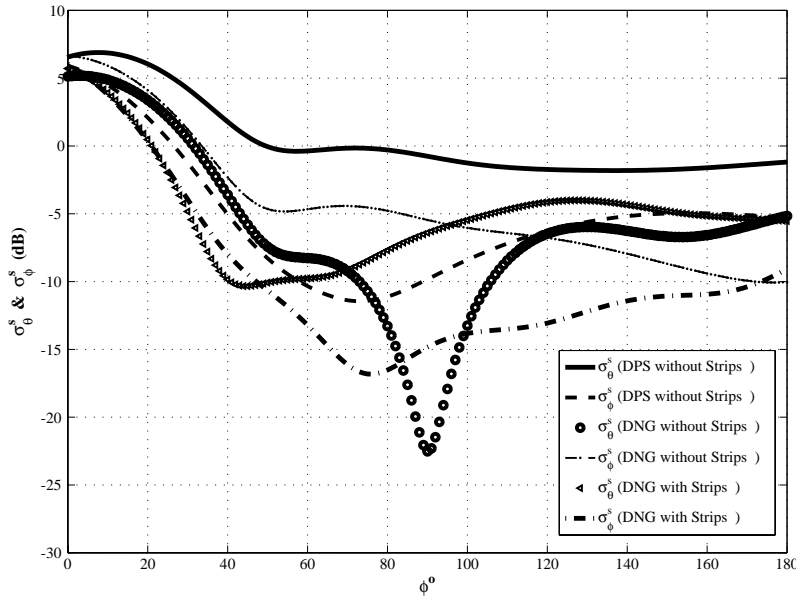


Figure 4. Scattered fields from a conducting cylinder coated with DPS and DNG material with/without 45° helical strips pitch angle under oblique incidence of $\theta_i = 60^\circ$ with polarization angle $\alpha = 45^\circ$.

results where the later term can be expressed in terms of the scattered and incident field components as:

$$\sigma = \lim_{\rho \rightarrow \infty} \left(2\pi\rho \frac{|E^s|^2}{|E^i|^2} \right) \tag{16}$$

where $|E^i|$ and $|E^s|$ are the scattered and the incident electric fields, respectively. It can be observed that the cross-polar component of the scattered field E_ϕ^s in the TM_z case and the E_θ^s in the TE_z polarization are equal. These results were expected and they agree totally with the phenomena stated in [9].

A number of parametric studies were conducted to demonstrate the behavior of MTM compared with normal conventional dielectric materials. It is important to examine the effect of having the helical strips compared with the scattering from a conducting cylinder coated with homogenous material of the same size with the approximation that the strip width asymptotically approaching to zero. Fig. 4 illustrates the scattering from conducting cylinder coated with both DPS and DNG materials with and without having helical aligned

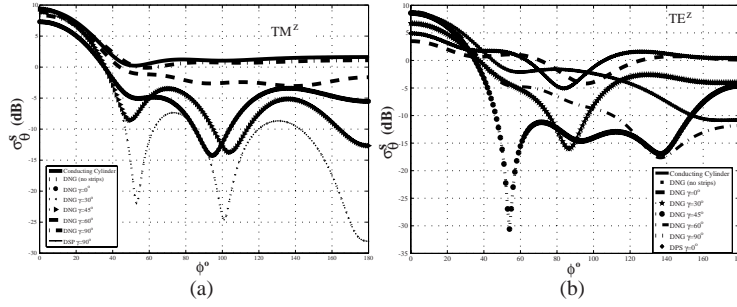


Figure 5. Scattered fields from a PEC cylinder coated with DPS/DNG homogenous layer with/without strips at different strips' pitch angle under normal incident of $\theta_i = 90^\circ$ compared with a 1.2 mm conducting cylinder radius. The coating cylinders have inner and outer coated layer radii of 1 mm and 1.2 mm, respectively. The coated material layer constitutive parameters are those in Table 2 for both polarizations (a) TM^z with $\alpha = 0^\circ$, (b) TE^z with $\alpha = 90^\circ$.

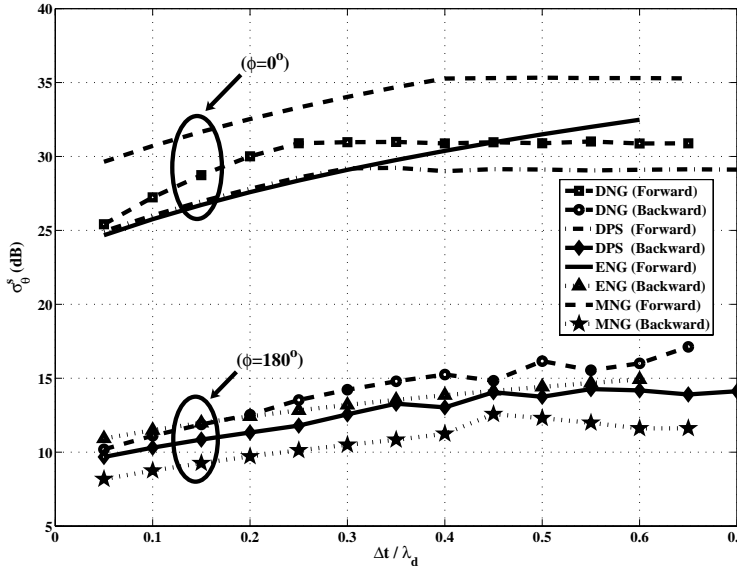


Figure 6. Effect of the electrical thickness of different coating materials on the forward and backward scattering waves under oblique incidence with helical strips rounded by pitch angle $\gamma = 45^\circ$.

strips of pitch angle $\gamma = 45^\circ$ under oblique incidence of $\theta_i = 60^\circ$ with polarization angle $\alpha = 45^\circ$.

Another study is developed to illustrate the influence of different

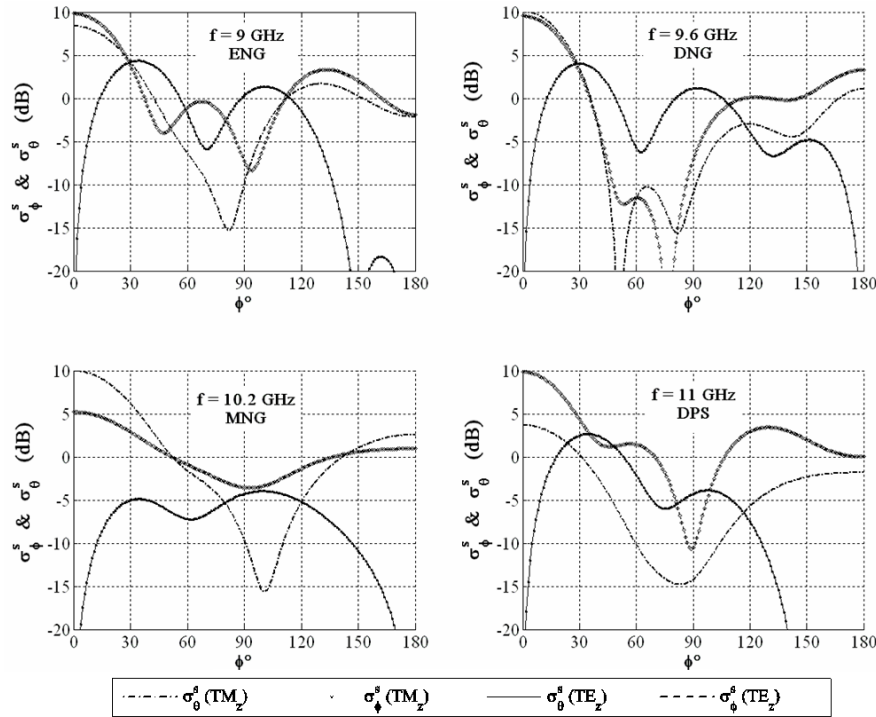


Figure 7. Scattering from a conducting cylinder coated with different materials and loaded with ϕ -directed strips under oblique incidence ($\theta_i = 45^\circ$).

strips' pitch angle loaded to conducting cylinder coated with metamaterials layer compared with the scattering from a conducting cylinder of the same size as shown in Fig. 5. The pitch angle is varying from 0° to 90° under normal incident with $\theta_i = 90^\circ$. The radius of the conducting cylinder is 1.2 mm while the radii in the coating cylinder case are $b = 1$ mm and $a = 1.2$ mm, respectively. Fig. 5(a) shows that for TM^z polarization, the scattered field from the conducting cylinder (PEC) is identical to the scattering from the cylinder with $\gamma = 90^\circ$ coated with DPS material and that agrees with results stated in [9] while scattering from DNG coated cylinder with no strips is identical to the scattering of DNG coated conducting cylinder with 0° pitch angle (ϕ -oriented strips). Fig. 5(b) presents similar behavior for TE^z polarization where the scattered field from a conducting cylinder is identical to the scattering from an ϕ -oriented PEC strips loaded to a conducting cylinder coated with DPS material with the same

size. Also, the scattering from the case where no strips are loaded is identical to that with z -oriented strips with DNG coating material. Both analysis and simulation results discussed previously demonstrate that scattering from the conducting cylinder coated with metamaterials and loaded with the strips arises promising properties compared with conventional dielectric material coating.

It is also interesting to determine the effect of the coating material's electrical thickness on the scattering performance for different materials. Fig. 6 illustrates both forward and backward scattering waves for different coating materials operating at different frequencies under oblique incident wave of $\theta_i = 45^\circ$, and $\phi_i = 0^\circ$ with polarization angle $\alpha = 45^\circ$.

It can be concluded that coating with metamaterials achieves enhancement in the forward scattering compared with the DPS materials. Longitudinal (z -directed) and circumferential (ϕ -directed) strip loading are examined with different coating materials as special cases of the helical strip loading. When $\gamma = 0^\circ$, the strips will be ϕ -directed and when $\gamma = 90^\circ$, the strips will be z -directed. Simulation results for the ϕ -directed case are shown in Figs. 7 for both TM_z and TE_z polarizations under oblique incidence with $\theta_i = 45^\circ$.

5. CONCLUSION

The scattering from a conducting cylinder coated with a conventional and metamaterials layer and loaded with conducting helical strips by using the ASBC under oblique incident plane waves was studied. The constitutive parameters of different material types were obtained with accordance to Drude-Lorentz material modeling formulas at different operating frequencies. The present work is proved to be valid implementation of the ASBC with other numerical techniques. Further code verifications were accomplished when both longitudinal (z -directed) and circumferential (ϕ -directed) strip loading were used as special cases for different polarizations and with normal and oblique incidence. A number of investigations were accomplished to have more knowledge about the benefits of using metamaterials a coating layers compared with the conventional dielectric media. A remarkable enhancement in the forward scattering was noticed with the existence of DNG materials with certain electrical thickness. The effect of the strip's pitch angle variation was also discussed for both TM_z and TE_z polarizations. This work presented the potential advantages of using the ASBC in modeling practical problems with different material configurations.

REFERENCES

1. Dragone, C., "New grids for improved polarization diplexing of microwaves in reflector antennas," *IEEE Trans. Antennas Propagat.*, Vol. 26, 459–463, Mar. 1978.
2. Hanfling, J. D., G. Jerinic, and L. R. Lewis, "Twist reflector design using E-type and H-type modes," *IEEE Trans. Antennas Propagat.*, Vol. 29, 622–629, July 1981.
3. Lier, E. and P.-S. Kildal, "Soft and hard horn antenna," *IEEE Trans. Antennas Propagat.*, Vol. 36, 1152–1157, 1988.
4. Lier, E., "Analysis of soft and hard strip-loaded horns using a circular cylindrical model," *IEEE Trans. Antennas Propagat.*, Vol. 38, 783–793, June 1990.
5. Kildal, P.-S., "Artificially soft and hard surfaces in electromagnetics," *IEEE Trans. Antennas Propagat.*, Vol. 38, 1537–1544, 1990.
6. Šipuš, Z., H. Merkel, and P.-S. Kildal, "Green's functions for planar soft and hard surfaces derived by asymptotic boundary conditions," *IEE Proc. - Microwave Antennas Propag.*, Vol. 144, No. 5, 321–328, October 1977.
7. Kildal, P.-S., A. A. Kishk, and A. Tengs, "Reduction of forward scattering from cylindrical objects using hard surfaces," *IEEE Trans. Antennas Propagat.*, Vol. 44, 1509–1520, Nov. 1996.
8. Kildal, P.-S., A. A. Kishk, and Z. Šipuš, "Asymptotic boundary conditions for strip-loaded and corrugated surfaces," *Microwave Opt. Technol. Lett.*, Vol. 14, 99–101, Feb. 1997.
9. Kishk, A. A. and P.-S. Kildal, "Asymptotic boundary conditions for strip-loaded scatterers applied to circular dielectric cylinders under oblique incidence," *IEEE Trans. Antenna Propagat.*, Vol. 45, No. 2, 551–557, USA, 1997.
10. Kishk, A. A. and P.-S. Kildal, "Asymptotic boundary conditions for strip-loaded surfaces of cylindrical structures with arbitrarily shaped cross-section," *IEEE Antennas and Propagat. Int. Symposium*, Vol. 2, 834–837, July 1999.
11. Kishk, A. A., "Analysis of hard surfaces of cylindrical structures of arbitrarily shaped crosssections using asymptotic boundary conditions," *IEEE Trans. Antenna Propagat.*, Vol. 51, 1150–1156, June 2003.
12. Engheta, N. and R. W. Ziolkowski, "A positive future for double-negative metamaterials," *IEEE Trans. Microwave Theory and Techniques*, Vol. 53, No. 4, 1535–1556, April 2005.
13. Ziolkowski, R. W., "Design, fabrication, and testing of double

- negative metamaterials,” *IEEE Trans. Antennas Propagat.*, Vol. 51, No. 7, 1516–1529, July 2003.
14. Engheta, N., “Metamaterials with negative permittivity and permeability: Background, salient features, and new trends,” *2003 IEEE MTT-S International Microwave Symposium Digest*, Vol. 1, 187–190, 2003.
 15. Shadrivov, I. V., A. A. Zharov, N. A. Zharov, and Y. S. Kivshar, “Nonlinear left-handed metamaterials,” *Radio Science*, Vol. 40, RS3S90, 2005.
 16. Jelinek, L., J. Machac, and J. Zehentner, “A magnetic metamaterial composed of randomly oriented SRRs,” *PIERS Online*, Vol. 2, No. 6, 624–627, 2006.
 17. Sihvola, A. H., P. Yla-Oijala, S. Jarvenpaa, and M. Taskinen, “Searching for electrostatic resonances in metamaterials using surface integral equation approach,” *PIERS Online*, Vol. 3, No. 1, 118–121, 2007.
 18. Lindell, I. V., S. A. Tretyakov, K. I. Nikoskinen, and S. Ilvonen, “BW media — Media with negative parameters, capable of supporting backward waves,” *Microwave and Optical Technology Letters*, Vol. 31, No. 2, 129–133, Oct. 2001.
 19. Valanju, P. M., R. M. Walser, and A. P. Valanju, “Wave refraction in negative-index media: always positive and very inhomogeneous,” *Physical Review Letters*, Vol. 88, No. 18, 012220, 2002.
 20. Smith, D. R. and N. Kroll, “Negative refractive index in left-handed material,” *Phys. Rev. Lett.*, Vol. 85, 2933, Oct. 2, 2000.
 21. Ziolkowski, R. W. and E. Heyman, “Wave propagation in media having negative permittivity and permeability,” *Physical Review Letter*, Vol. 64, 056625, 2001.
 22. Pendry, J. B., “Negative refraction,” *Contemporary Physics*, Vol. 45, No. 3, 191–203, 2004.
 23. Veselago, V. G., “The electrodynamics of substances with simultaneously negative values of ϵ and μ ,” *Soviet Physics Uspekhi*, Vol. 10, No. 4, 509–514, 1968. (In Russian, *Usp. Fiz. Nauk*, Vol. 92, 517–526, 1967).
 24. Zharov, A. A., I. V. Shadrivov, and Y. S. Kivshar, “Nonlinear properties of left-handed metamaterials,” *Physical Review Letters*, Vol. 91, No. 3, 03740121–03740124, Mar. 2003.
 25. Liang, L., B. Li, S.-H. Liu, and C.-H. Liang, “A study of using the double negative structure to enhance the gain of rectangular waveguide antenna arrays,” *Progress In Electromagnetics Re-*

- search, PIER 65, 275–286, 2006.
26. Caloz, C. and T. Itoh, “Transmission line approach of left-handed (LH) materials and microstrip implementation of an artificial LH transmission line,” *IEEE Trans. Microwave Theory Tech.*, Vol. 52, 1159–1166, May 2004.
 27. Mittra, R., K. Rajab, and M. T. Lanagan, “Size reduction of microstrip antennas using metamaterials,” *Proc. IEEE AP-S*, Washington, DC, July 2005.
 28. Erentok, A. and R. W. Ziolkowski, “Development of epsilon negative (ENG) metamaterials for efficient electrically small antenna applications,” *Proc. IEEE AP-S*, Washington, DC, July 2005.
 29. Pendry, J. B., “Negative refraction makes a perfect lens,” *Physics Review Letter*, Vol. 85, No. 18, 3966–3969, 2000.
 30. Lagarkov, A. N., V. N. Kisel, and V. N. Semenenko, “Wide-angle absorption by the use of a metamaterial plate,” *Progress In Electromagnetics Research Letters*, Vol. 1, 35–44, 2008.
 31. Henin, B. H., M. H. Al Sharkawy, and A. Z. Elsherbeni, “Scattering of obliquely incident plane wave by an array of parallel concentric metamaterials cylinders,” *Progress In Electromagnetics Research*, PIER 77, 285–307, 2007.
 32. Valagiannopoulos, C. A., “Electromagnetic scattering from two eccentric metamaterial cylinders with frequency-dependent permittivities differing slightly each other,” *Progress In Electromagnetics Research B*, Vol. 3, 23–34, 2008.
 33. Zainud-Deen, S. H., A. Z. Botros, and M. S. Ibrahim, “Scattering from bodies coated with metamaterial using FDTD method,” *Progress In Electromagnetics Research B*, Vol. 2, 279–290, 2008.
 34. Li, C. and Z. Shen, “Electromagnetic scattering by a conducting cylinder coated with metamaterials,” *Progress In Electromagnetics Research*, PIER 42, 91–105, 2003.
 35. Shooshtrai, A. and A. R. Sebak, “Electromagnetic scattering by parallel metamaterial cylinders,” *Progress In Electromagnetics Research*, PIER 57, 165–177, 2006.
 36. Henin, B. H., A. Z. Elsherbeni, and M. H. Al Sharkawy, “Oblique incidence plane wave scattering from an array of circular dielectric cylinders,” *Progress In Electromagnetics Research*, PIER 68, 261–279, 2007.
 37. Ragheb, H. A. and M. Hamid, “Scattering by N parallel conducting circular cylinders,” *Int. J. Electron.*, Vol. 59, 407–421, Jan. 1985.

38. Hamid, A. K. and M. I. Hussein, "Iterative solution to the electromagnetic plane wave scattering by two parallel conducting elliptic cylinders," *Journal of Electromagnetic Waves and Applications*, Vol. 17, 813–828, 2003.
39. Kim, C. S., "Scattering of an obliquely incident wave by a coated elliptical conducting cylinder," *Journal of Electromagnetic Waves and Applications*, Vol. 5, No. 11, 1169–1186, 1991.
40. Smith, D. R., S. Schultz, P. Markos, and C. M. Soukoulis, "Determination of effective permittivity and permeability of metamaterials from reflection and transmission coefficients," *Phys. Rev. B*, Vol. 65, 195104:1–5, 2002.
41. Ishimaru, A., S.-W. Lee, Y. Kuga, and V. Jandhyala, "Generalized constitutive relations for metamaterials based on the quasi-static Lorentz theory," *IEEE Trans. Antennas Propagat.*, Vol. 51, 2550–2557, October 2003.
42. Lubkowski, G., R. Schuhmann, and T. Weiland, "Extraction of effective metamaterial parameters by parameter fitting of dispersive models," *Microwave and Optical Technology Letters*, Vol. 49, No. 2, Feb. 2007.
43. Smith, D. R., W. J. Padilla, D. C. Vier, S. C. Nemat-Nasser, and S. Schultz, "A Composite medium with simultaneously negative permeability and permittivity," *Phys. Rev. Lett.*, Vol. 84, 4184, 2000.
44. Markös, P. and C. M. Soukoulis, "Transmission properties and effective electromagnetic parameters of double negative metamaterials," *Optics Express*, Vol. 11, No. 7, April 7, 2003.
45. Smith, D. R., D. C. Vier, W. Padilla, S. C. Nemat-Nasser, and S. Schultz, "Loop-wire medium for investigating plasmons at microwave frequencies," *Appl. Phys. Lett.*, Vol. 75, 1425–1427, 1999.
46. Tretyakov, S. A., I. S. Nefedov, C. R. Simovski, and S. I. Maslovski, "Advances in electromagnetics of complex media and metamaterials," *NATO-ARW Proceedings*, Kluwer, 2002.
47. P. Markös and C. M. Soukoulis, "Transmission studies of the left-handed materials," *Phys. Rev. B*, Vol. 65, 033401, 2002.
48. Bohren, C. and D. Huffmann, *Absorption and Scattering of Light by Small Particles*, John Wiley, New York, 1983.
49. Jackson, J. D., *Classical Electrodynamics*, John Wiley, New York, 1999.